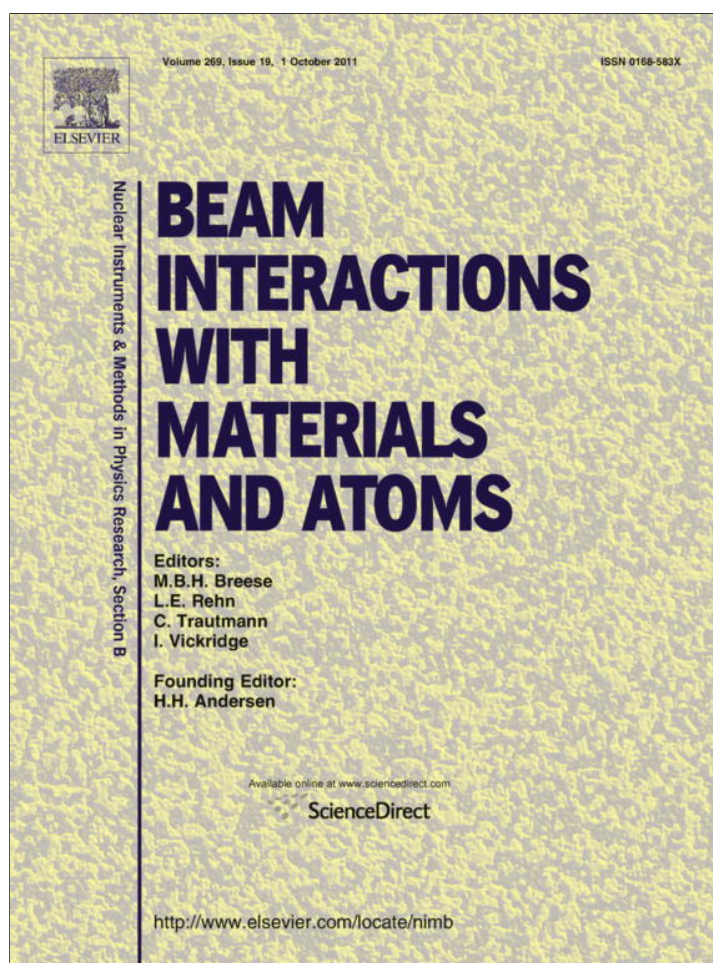


Provided for non-commercial research and education use.
Not for reproduction, distribution or commercial use.



This article appeared in a journal published by Elsevier. The attached copy is furnished to the author for internal non-commercial research and education use, including for instruction at the authors institution and sharing with colleagues.

Other uses, including reproduction and distribution, or selling or licensing copies, or posting to personal, institutional or third party websites are prohibited.

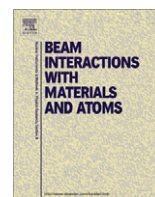
In most cases authors are permitted to post their version of the article (e.g. in Word or Tex form) to their personal website or institutional repository. Authors requiring further information regarding Elsevier's archiving and manuscript policies are encouraged to visit:

<http://www.elsevier.com/copyright>



Contents lists available at ScienceDirect

Nuclear Instruments and Methods in Physics Research B

journal homepage: www.elsevier.com/locate/nimb

A new method to combine IBA of fine aerosols with Radon-222 to determine source characteristics

Jagoda Crawford*, David D. Cohen, Wlodek Zahorowski, Scott Chambers, Eduard Stelcer

Australian Nuclear Science and Technology Organisation, Locked Bag 2001, Kirrawee DC NSW 2232, Australia

ARTICLE INFO

Article history:

Received 16 January 2011
Received in revised form 8 June 2011
Available online 2 July 2011

Keywords:

Ion beam analysis
PIXE
Radon
Fine particles

ABSTRACT

Accelerator based ion beam analysis (IBA) techniques were used to determine the elemental composition of aerosol samples from four sites near Sydney, Australia. Hourly measurements of atmospheric Radon-222 (radon) concentration were made at the same sites. We evaluate a new method for quantifying the degree of distribution of aerosol sources based on the correlation analysis of two consecutive years (2007–2008) of IBA and radon data.

Seasonal cycles and trends in concentrations of key elemental constituents of the sampled aerosols are characterised, and explained in terms of the regional Sydney climatology and proximity of measurement sites to the coast. Site-to-site correlation analysis was then undertaken between elements to quantify the extent to which a source had a regional impact or was only local to a site (site-specific). This was followed by correlation analysis of elements and radon at each site to identify the degree of spatial and temporal uniformity of the source at each site.

Silicon concentrations (usually associated with soil sources), were overall well correlated between three of the four sites, indicative of a regional source for three sites and a local source for the fourth site. Conversely, the highest sulfur correlations were observed between sites that were closest together.

On a site-by-site basis, radon was well correlated with black carbon and potassium and particularly during winter when domestic heating constitutes a distributed source. However, in summer the correlation of radon with BC and K was poor indicating that the distribution of these sources varies over the summer fetch region. Radon was also positively correlated with silicon and titanium, but the correlation coefficient for the entire data set was smaller than for black carbon. In summer and winter, when fetch regions were constrained by the prevailing meteorology, silicon and titanium showed a better correlation with radon. A small negative correlation was seen between sodium (a marker for sea salt) and radon.

Crown Copyright © 2011 Published by Elsevier B.V. All rights reserved.

1. Introduction

Sydney is Australia's largest city (4.4 million inhabitants in 2009) and continues to expand. Between 2000 and 2009 its population increased by more than 7%, and in 2008 alone the Sydney region released 2680 kT of gaseous and particulate emissions into the atmosphere [1]. The current study covers three airsheds (Fig. 1a): Hunter airshed north of Sydney, Illawarra airshed south of Sydney and the Sydney airshed.

The Sydney airshed, into which the majority of its urban emissions feed, is clearly delineated by the topographic confines of the Great Dividing Range; which rises to over 1000 m above sea level to the west, and 200 m to the north and south, enclosing a coastal plain approximately 70 km wide. The ongoing problem with photochemical smog and its precursors within the Sydney airshed indicates that the city's growing resource demand is more than

offsetting the continual improvements being made to fuels, motor vehicles and industry [2].

In addition to the numerous "diffuse emitters" (mobile sources, scattered small industries and non-industrial sources), the Hunter airshed plays host to open-cut coal mines and several coal fired power stations. A number of significant point sources are also present in the Sydney airshed including the Kurnell Oil Refinery. The Port Kembla Industrial site is located in the Illawarra airshed near Warrawong (Fig. 1b). As well as the growing smog concerns, dust and other particulate matter (e.g. wood smoke), continue to be a problem in some western areas of the Sydney airshed [2].

The synoptic wind flow patterns are typically onshore in summer and offshore in winter [3,4]. The climatology of photochemical smog and related gaseous emissions in the Sydney region has been studied extensively over the past 40 years [4–7]. A common finding was that Sydney is most prone to photochemical smog events in summer, with the severity of events linked to the prevailing winds and cloud cover.

* Corresponding author. Tel.: +61 2 9717 3885; fax: +61 2 9717 9260.

E-mail address: Jagoda.Crawford@ansto.gov.au (J. Crawford).

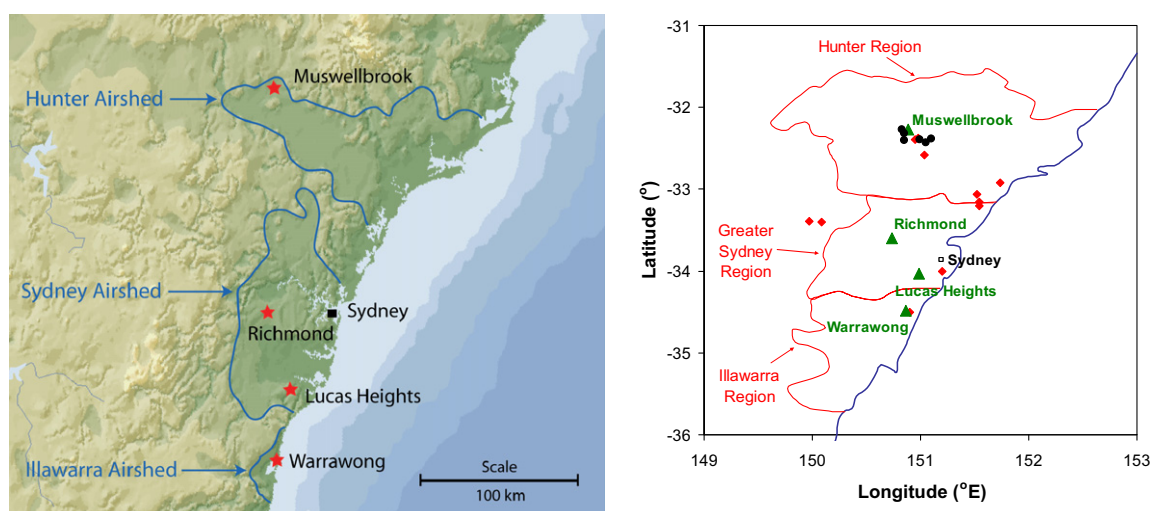


Fig. 1. (a) Topographic map of the study domain indicating the measurement sites and the Sydney, Hunter and Illawarra airsheds, and (b) map of the study domain showing regional boundaries (red lines), sampling sites (green triangles), and locations of major aerosol point sources (red diamonds) and open-cut coal mines (black circles). (For interpretation of the references to colour in this figure legend, the reader is referred to the web version of this article.)

Many aerosol characterisation investigations in Sydney, including those using nuclear methods, have been published in the last 15 years [4,8–13]. Aerosol pollution, particularly from particles smaller than $10\ \mu\text{m}$ in diameter, is associated with the growing problem of “brown haze”. Conditions conducive to brown haze (heavy particulate loading, low wind speed and shallow inversion layers), are most common in autumn and winter. Typically, the sources of these aerosols are motor vehicles, open fires, domestic combustion heaters, industry and soil. At higher concentrations these aerosols pose both direct and indirect risks (e.g. public health and visibility) and concern has recently focused on the fine particulate matter ($\text{PM}_{2.5}$), which is known to be linked more directly to adverse health effects than coarser matter [14]. Mobile sources contribute around 18% of Sydney’s $\text{PM}_{2.5}$ emissions, compared to 40% from industries and 42% from commercial and residential sources [11]. In the summer months, bushfires also contribute to the existing anthropogenic $\text{PM}_{2.5}$ loadings. During winter, wood heaters can produce up to three times more particulate pollution than cars [15]. Accelerator-based ion beam analysis (IBA) techniques have previously been used to characterise the elemental composition of fine particles and both source fingerprints and their contributions to the total mass have been quantitatively determined [16–19].

Radon is a ground-emitted and chemically stable gas. Terrestrial sources of radon are relatively constant on regional spatial scales and sub-seasonal time scales [20]. Furthermore, radon emissions from ice-free, unsaturated soils are typically three orders of magnitude greater than marine sources [21,22], making it an ideal tracer of recent (in the order of 3-weeks) terrestrial influence on an air mass [23]. Largely due to its comparatively simple atmospheric source-sink mechanisms, radon has long been recognised as a useful tracer of atmospheric transport [24–26]. As well as providing unambiguous evidence of recent terrestrial influence, changes in radon concentration measured near the surface on sub-diurnal time-scales also reflect the effects of dilution due to variations in the depth of the atmospheric boundary layer.

The application of IBA for the elemental composition of aerosols, and then using radon and back trajectories for source region analysis, has recently been reported by Crawford et al. [27,28] for a study site in Hong Kong. The primary aims of the current study were: (i) to contrast 2 years of daily elemental composition of $\text{PM}_{2.5}$ aerosols, and their seasonal variability, from four sites in the greater Sydney region, and (ii) to use the new technique, that of correlation between elemental markers of various $\text{PM}_{2.5}$

pollution types and observed atmospheric radon concentrations at each site, and together with site-to-site correlation of elements to infer spatial characteristics of the pollution sources.

For the two year study period (2007–2008), the southern hemisphere definition of seasons has been employed: summer (December, January and February), autumn (March, April and May), winter (June, July and August) and spring (September, October and November).

2. Method

2.1. Sites and study domain

The four sampling sites (Warrawong, Lucas Heights, Richmond and Muswellbrook) and main regional airsheds are shown in Fig 1. As well as representing a north–south cross section through the airsheds, these sites are at increasing distance from the coast (3–130 km), providing a progressive reduction in marine influence.

The Warrawong site (WW; $34^{\circ}29'S$, $150^{\circ}52'E$; 40 m asl) is 3 km from the coast. Since it is south-west of the Port Kembla industrial complex, it is classified as an urban/heavy industrial site. Major industries in this area include ferrous metal smelting and refining plant, a large integrated steelworks (coke ovens, sinter plant and blast furnace) together with iron ore, coal and grain handling facilities [29]. The Lucas Heights site (LH; $34^{\circ}02'S$, $150^{\circ}59'E$; 152 m asl) is 18 km from the coast, and situated on a broad ridge with drops in elevation of 130–150 m within a 1 km radius. LH is classified as a rural/urban site. In terms of marine influence on observed aerosols, both WW and LH will hereafter be classified as “coastal sites”.

The Richmond site (RI; $33^{\circ}36'S$, $150^{\circ}44'E$; 24 m asl) is 55 km from the coast. It is located in a relatively flat area near the western boundary of the Sydney airshed. Muswellbrook (MB; $32^{\circ}16'S$, $150^{\circ}53'E$; 144 m asl) is 130 km from the coast and in a broad valley. MB is situated near open-cut coal mines and two coal-fired power stations. Both RI and MB are classified as rural/industrial sites. In terms of marine influence on observed aerosols, both RI and MB will hereafter be classified as “inland sites”.

2.2. Aerosol sampling and elemental analysis

Aerosols were sampled using an IMPROVE $\text{PM}_{2.5}$ cyclone system, with a 25 mm diameter Teflon filter and flow rate of

~22 L min⁻¹ [16]. 24-h integrated samples (midnight to midnight) were collected twice a week (Wednesday and Sunday). However, since no significant difference was noted between samples collected on weekdays and weekends, all days have been used in the following analysis.

Elemental analysis of the sampled aerosols was performed using accelerator-based ion beam analysis (IBA) techniques [17,18], which yielded quantitative concentrations for the following elements: H, Na, Al, Si, P, S, Cl, K, Ca, Ti, V, Cr, Mn, Fe, Co, Ni, Cu, Zn, Br and Pb. The full suite of analyses included: Proton-induced X-ray Emission (PIXE), Proton-induced Gamma-ray Emission (PIGE), Rutherford Backscattering (RBS) and Proton Elastic Scattering Analysis (PESA).

Characterisation of detailed source fingerprints for Sydney's PM_{2.5} pollution is beyond the scope of this investigation and is the subject of a separate study. Instead, here we consider combinations of key elements understood to be markers of different source types [4,27,19,30], namely: the Si–Ti pair, which is an effective marker for Australian soils [19]; the Black Carbon (BC)–K pair, which is generally a good indicator of smoke (although BC is also present in vehicle exhaust); the Fe–Zn pair, an indicator of heavy industry emissions (although Zn is also associated with motor vehicles); the Na–Cl pair, consistent with sea spray, an indicator of marine influence (although Cl is often depleted in transit by reaction with acidic species and other sources of Cl might also exist); and particulate sulfur (S), which is typically in the form of secondary sulfate, produced by the conversion of SO₂ gas to the particulate sulfate phase in the presence of sunlight and water vapour [31]. SO₂ can have a range of sources, including vehicles, coal fired power plants and other industrial activity.

2.3. Atmospheric radon measurements

The naturally occurring radioactive gas Radon-222 (radon; half life $t_{0.5} = 3.82$ days) is chemically inert and poorly soluble in water. Its parent, radium-226, is long lived ($t_{0.5} = 1600$ years) and ubiquitous to all terrestrial surfaces. Terrestrial radon flux densities typically range from 16 to 26 mBqm⁻² s⁻¹; [32,33] and are considered to be relatively consistent on regional spatial scales and sub-seasonal time scales (e.g. Jacob et al. [20]).

Continuous, hourly measurements of atmospheric radon concentration were made concurrently with aerosol sampling at each of the four sites during the whole study period. The radon measurements were made using 1500 L dual flow loop, two filter detectors [34].

2.4. Source characterisation by correlation analysis

The degree of site-to-site correlation between corresponding elemental concentrations can be used to indicate whether a particular source is regional (i.e. large-scale) or local (i.e. small-scale and close to a particular site). For example, a good correlation between sites is consistent with a regionally distributed source [35,36]. Conversely, low inter-site correlations would be expected if sources were local with respect to a given site (site-specific) [37].

In addition to the site-to-site correlations the correlation between radon and elemental concentrations at a given site is related to how similar (or otherwise) the characteristics of the aerosol source match those of radon (i.e. exclusively terrestrial, large scale, as well as spatially and temporally uniform).

2.5. Back trajectory calculation

Air mass back trajectories have been used in conjunction with atmospheric radon measurements to assist with the interpretation of observed seasonal changes in aerosol characteristics. Back tra-

jectories were generated using the PC version of HYSPLIT v4.0 (Hybrid Single-Particle Lagrangian Integrated Trajectory [38]). When calculating the back trajectories, two starting heights were considered, 50 and 500 m above ground level. Since little difference was noted only the 50 m results are shown. In comparing HYSPLIT calculated trajectories with tracer gas releases, Draxler [39] estimated that the model error is between 20% and 30% of the travel distance. Consequently we have restricted back trajectories to 5 days. The chosen length is adequate for delineation of the main fetch areas.

3. Results and discussion

3.1. Elemental concentrations, seasonal variation and site-to-site correlation

3.1.1. Seasonal fetch analysis using back trajectories

Seasonal changes in regional meteorology are responsible for redistributing Sydney's PM_{2.5} burden on sub-annual time scales. To facilitate the interpretation of seasonal trends in aerosol concentration fetch analyses were performed for each site using back trajectories. To do this, hourly back trajectories were calculated for the 2-year period and seasonal density plots were generated by counting the number of times that a grid cell (of 0.5° × 0.5° resolution) was crossed by a trajectory in that season. The result was a frequency distribution of air mass passage over the potential aerosol fetch regions. Separate density plots were generated for each site and season but, since results were similar for both coastal sites and both inland sites, only plots for the domain extremes (WW, Fig. 2; MB, Fig. 3) will be shown.

In winter (Figs. 2b and 3b), air parcels typically approached each site from the west or south-west, having crossed southeast Australia (terrestrial fetch, or “off-shore” flow). In summer (Figs. 2d and 3d), air masses typically approached the sites from the northeast to southeast quadrant, and exhibited comparatively short land fetches (marine fetch, or “on-shore” flow). Autumn and spring were characterised by mixed fetch conditions.

Irrespective of season the inland sites had a greater terrestrial fetch. While this is evident from Figs. 2 and 3 (particularly in summer) it is better quantified by the time-over-land estimates in Table 1. Consequently, in summer, despite the prevailing easterly winds, the inland sites (MB in particular), may have a significant terrestrial signature from near coastal regions. However, for all sites, air masses spend more time over land in winter than in summer. Since the majority of aerosols have terrestrial based sources the potential for high pollution episodes, given similar emissions rates, should be highest in winter. However, for the inland sites the most heavily populated regions are the coastal plains to the east of the sites, which points to higher significance of the coastal regions in summer, especially for anthropogenic pollutions.

3.2. Elemental concentrations

Time series of daily average concentrations (ng/m³) of select elements (Na, Si, S, K and BC) are presented in Figs. 4–8, respectively. Corresponding plots for Cl, Ti, Fe and Zn are provided as supplementary data. In some cases a clear seasonal cycle is evident, and/or a trend with increasing distance from the coast. On inspection the degree of correlation of these cycles and trends between sites can be seen to change with each element. This is explored in more detail in Section 3.1.3.

The seasonality and trends in marine influence, of observed elemental concentrations is more clearly evident when the data are plotted as seasonal averages (Fig. 9). This figure also highlights some anomalies at WW and MB which, most likely, result from their proximity to strong point sources.

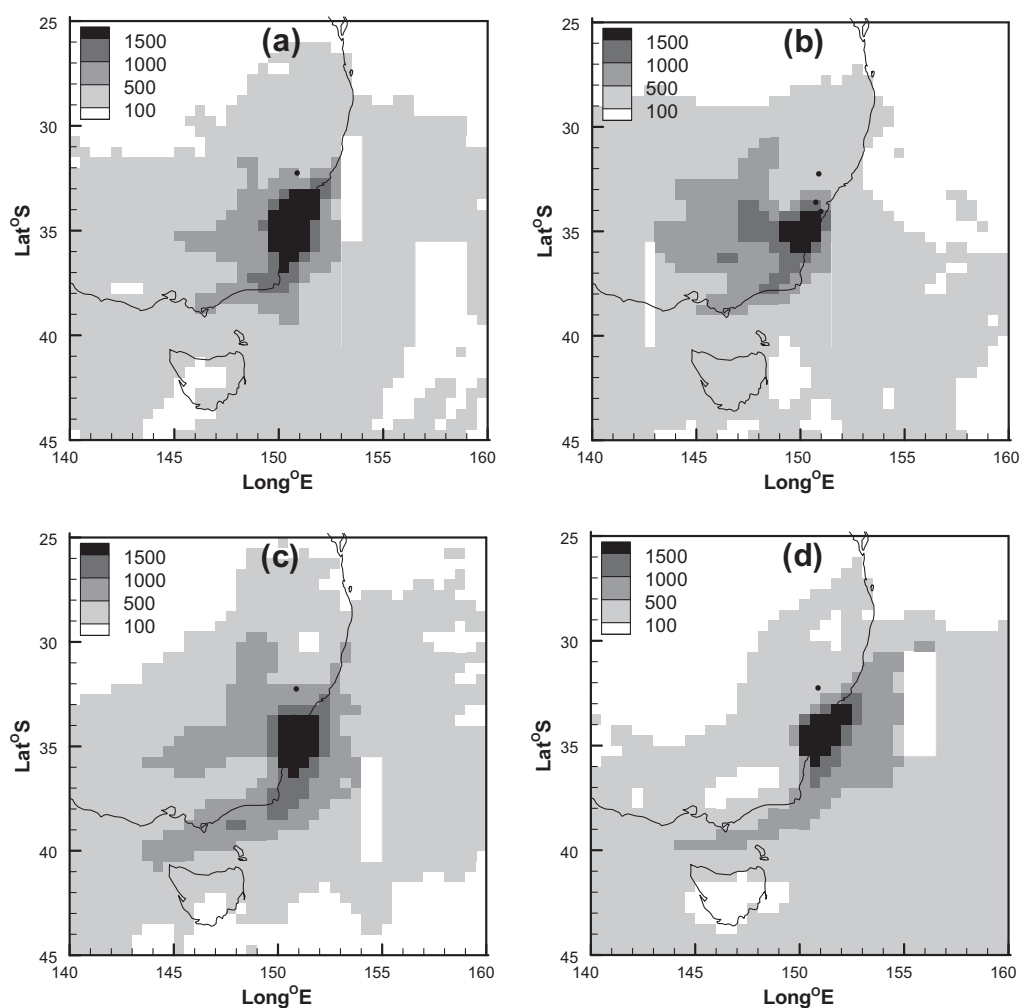


Fig. 2. Trajectory density plots (number of trajectories passing over a $0.5^\circ \times 0.5^\circ$ grid cell) for Warrawong in: (a) autumn, (b) winter, (c) spring and (d) summer, also representative of the coastal site Lucas Heights.

3.2.1. Marine influence (Na–Cl pair)

Overall a pronounced reduction in marine markers was evident with increasing distance from the coast (Fig. 9a and b). A strong seasonality in marine markers was also noted, consistent with the seasonal change in prevailing wind direction from “onshore” (summer) to “offshore” (winter). Higher concentrations of marine markers in spring than autumn were also consistent with trajectory density plots (Figs. 2 and 3) and time-over-land estimates (Table 1). On examination of the scatter plots of Cl against Na (not presented) it was found that for RI 22% of winter measurements were above the Cl/Na ratio of 1.54 (a ratio for sea spray [16]), an indication of local sources of Cl to the south-west consistent with the winter fetch.

3.2.2. Australian soil markers (Si–Ti pair)

Concentrations of Si and Ti were highest at MB for all seasons (Fig. 9d and e), indicative of a distinctive soil source for this site. MB receives more soil from the summer onshore winds than from the winter westerlies. This can be attributed to three factors; (a) in MB rural land is located to the east down the Hunter Valley, which is a possible source region, (b) a number of open-cut mines are located to the south/south-east of MB (Fig. 1) which are probably the most significant contributor, and (c) native forests are located to the south-west resulting in a reduced dust source. With one exception (Ti at WW in summer), the strongest soil signatures were observed in autumn and spring.

3.2.3. Smoke markers (BC–K pair)

Concentrations of K and BC showed less variability between the sites (Fig. 9g and h). Contrasting seasonal cycles were observed between WW and RI, with the highest concentration at WW in spring and summer, and highest concentration at RI in autumn and winter. Since RI is a semi-rural site, fossil fuel burning (for heating) and biomass burning (for clearing/waste removal) are prevalent in winter. Throughout the non-winter months WW was downwind of the Port Kembla industrial facility for a significant fraction of time, resulting in higher K concentrations. No trend in K or BC was observed with distance from the coast based on seasonal averages or from the time series (Figs. 7–9). Minimum values for both smoke markers were recorded at LH, a site that is affected predominantly by urban sources.

3.2.4. Heavy industry markers (Fe–Zn pair)

The highest concentrations of Fe and Zn (Fig. 9f and i) were recorded at WW, attributed to the adjacent industrial activity east of the site. The seasonal cycle of both these markers at WW was characterised by spring/summer highs and autumn/winter lows. In the case of Zn concentrations, a weak seasonal cycle was evident for all three remaining sites.

3.2.5. Particulate (secondary) S

Concentrations of S were slightly higher in WW year round (Fig. 7c). In all cases however, a clear seasonal cycle was evident,

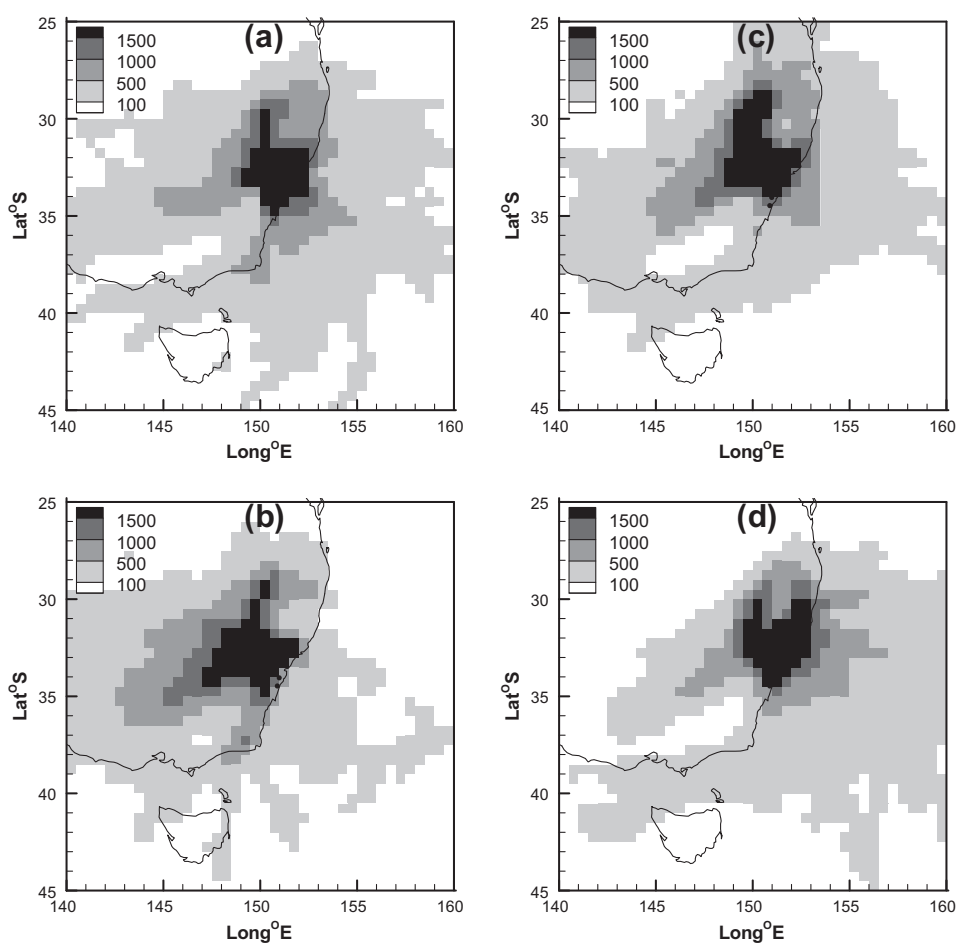


Fig. 3. Trajectory density plots (number of trajectories passing over a $0.5^\circ \times 0.5^\circ$ grid cell) for Muswellbrook in: (a) autumn, (b) winter, (c) spring and (d) summer, also representative for the inland site Richmond.

Table 1

Seasonal average time over land (days) for air masses before arriving at the coastal and inland measurement sites (calculated for those days on which aerosol measurements were available).

Season	Coastal sites	Inland sites
Autumn	1.4	1.9
Winter	1.9	2.5
Spring	1.2	2.2
Summer	0.7	1.5

which was characterised by low concentrations in winter (south-west fetch, mainly rural) and high concentrations in other seasons (coastal/urban fetch). Assuming that the majority of S collected represents secondary aerosols, this seasonality is also consistent with there being less sunlight in the winter months for the conversion of SO_2 to particulate sulphate, however the change in fetch regions could also be a factor. Based on measurements of incoming shortwave radiation made at LH, the daily total clear sky insolation in June is approximately $11.45 \text{ MJ/m}^2/\text{day}$ compared to equivalent December values of $31.11 \text{ MJ/m}^2/\text{day}$.

3.3. Site-to-site elemental correlation

Site-to-site correlations of Na (the preferred marine marker) were typically significant and positive (Table 2; see also Fig. 4), indicating a common, widespread/regional source (the adjacent ocean). The site-to-site correlations of radon are significant

(typically larger than for Na) and positive, since the source is terrestrial and relatively uniform in space and time. Since both the ocean and terrestrial sources are extensive, one interpretation of the difference in correlation magnitudes of Na and radon is that the removal rates of sea-spray aerosols are faster than the removal (radioactive decay) of radon.

Site-to-site S correlations were typically larger in winter than summer, despite S concentrations having a winter minimum (Fig. 9), so the winter S source is most likely distant and well mixed in the lower atmosphere to influence all sites. In summer, site-to-site S correlations are lowest between MB and other sites, indicating that sources of secondary sulphate in the Hunter Valley are largely site-specific. Given the easterly fetch in summer this is consistent with a source in the industrialised Newcastle region and/or the coal fired power stations to the south-east. LH and RI were well correlated in summer and winter (see also Fig. 6), indicating that secondary sulphates resulting from the urban Sydney plume were fairly well mixed within the Sydney airshed.

Site-to-site correlations of the smoke markers (K and BC) were lower, with the highest values occurring between sites that were closest together, indicating that most K and BC sources were site-specific. K and BC correlations may be artificially high in winter though since smoke concentrations will increase at all sites under stable atmospheric conditions irrespective of source location.

The high site-to-site correlation of Si (soil marker) between three of the sites (WW, LH and RI) indicates a common and widespread source. Si correlations were poorest with MB, which is known to have strong site-specific soil sources (open-cut mines and agriculture).

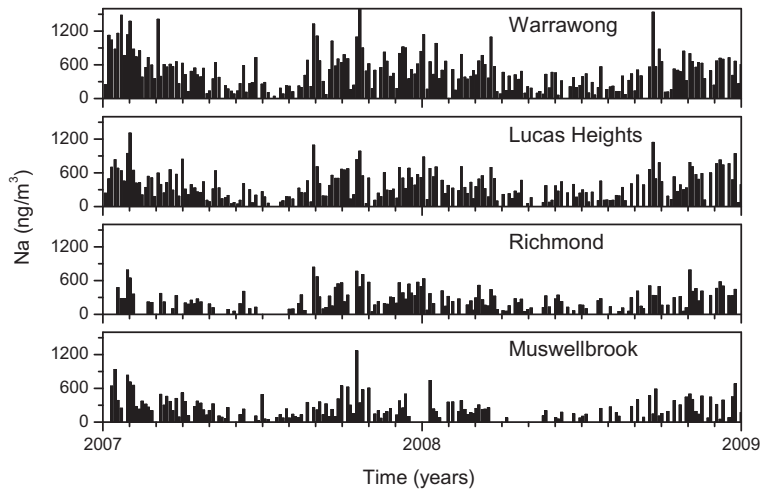


Fig. 4. Time series of Na, for 2007 and 2008, at the four sites.

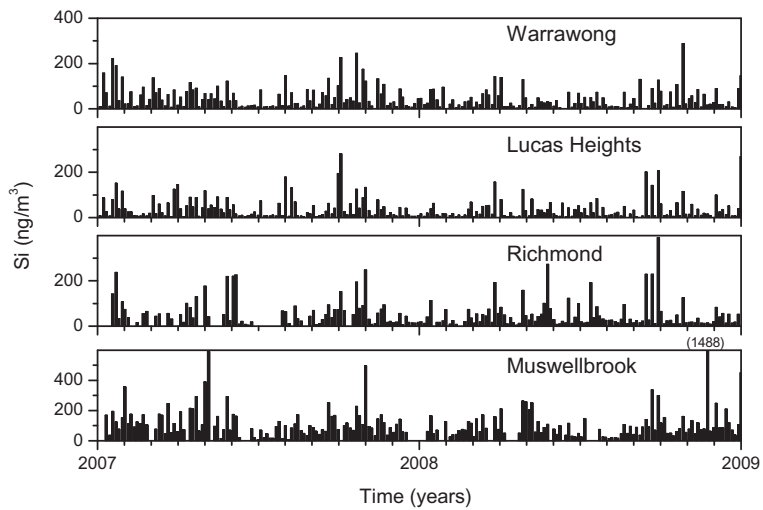


Fig. 5. Time series of Si, for 2007 and 2008, at the four sites. Note the difference in the y-scale for Muswellbrook. Also note a large peak was recorded in Muswellbrook in spring 2008 with its height shown in brackets.

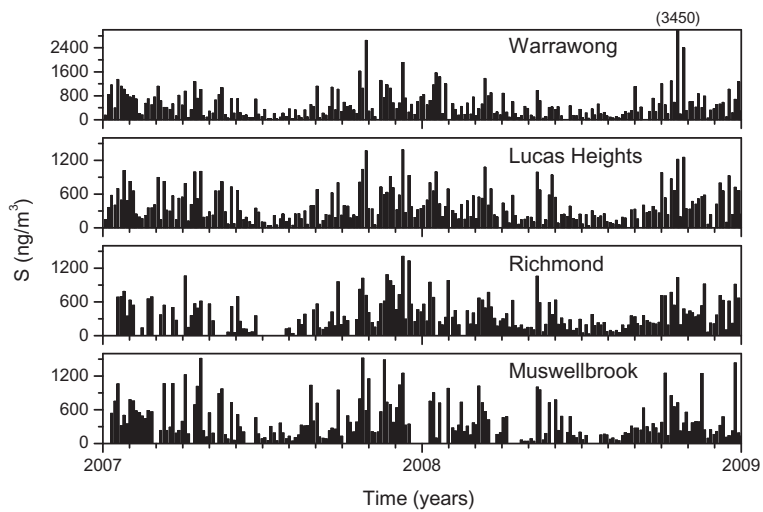


Fig. 6. Time series of S, for 2007 and 2008, at the four sites. Note the difference in the y-scale for Warrawong.

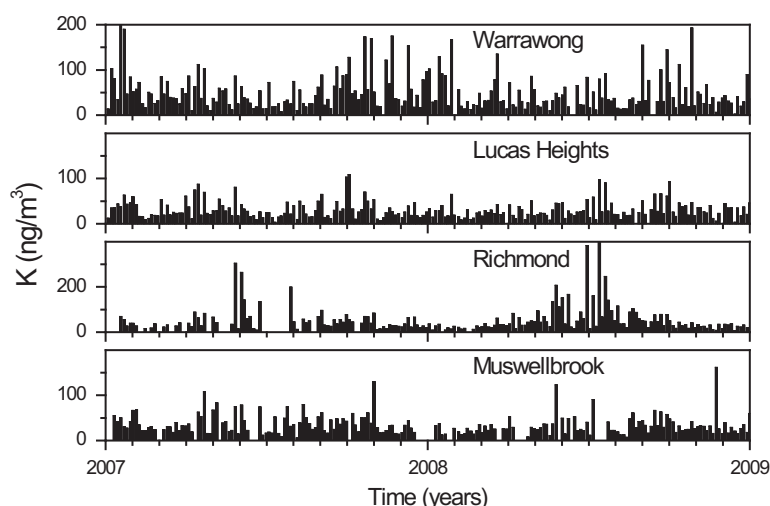


Fig. 7. Time series of K, for 2007 and 2008, for the four sites. Note the difference in the y-scale for Richmond.

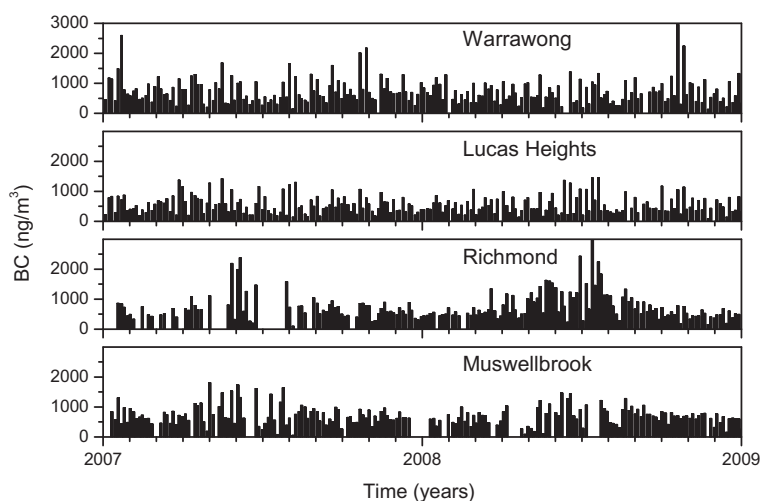


Fig. 8. Time series of BC, for 2007 and 2008, at the four sites.

3.4. Seasonality of observed radon concentrations

The time series of the daily mean radon, for those days on which aerosol samples were available, are presented in Fig. 10. The aerosol concentrations are the daily mean concentrations in the atmosphere, whereas, radon is hourly averaged. For comparison with aerosol measurements a daily mean radon activity is calculated and used.

Daily mean radon concentrations were highest for the inland sites and lowest for the coastal sites. Although LH was further inland than WW, the site is situated on a local topographic high point, resulting in smaller nocturnal maxima and corresponding daily means.

All sites exhibited a pronounced seasonality in mean radon, characterised by a summer minimum (when onshore flow results in a short land fetch) and higher concentrations in autumn and winter (when longer air mass time over land is recorded; Table 1).

Time over land alone, however, is not an indicator of the degree of coupling between air masses and the land surface, since air masses could spend a significant proportion of their time above the planetary boundary layer, removed from the surface source. The coupling of an air mass with the land surface, and hence the potential for entrainment of emissions from surface sources, can

be gauged by the measured radon activity. Seasonal average radon activity is presented in Table 3, indicating that, at each site, summer air masses have the least terrestrial influence and the largest terrestrial influence is seen in autumn.

3.5. Investigating the correlation between aerosols and radon

Below we present and discuss correlations between radon and selected elements for (a) the dataset grouped by degree of terrestrial influence as determined by radon concentration, and (b) the dataset as a whole. Daily mean radon has been used for this analysis to match the 24-h aerosol sampling period.

3.6. Terrestrial influence on aerosol loading

Since, for the purpose of this study, radon can be considered to have an exclusively terrestrial source, we grouped the aerosol samples according to quartiles of radon concentration to represent degrees of terrestrial influence on air mass composition. Here we focus the discussion on Group 1, being the quarter of the data with the least amount of radon, representing the lowest terrestrial influence and Group 2, being the quarter of the data with the highest radon, representing the highest terrestrial influence.

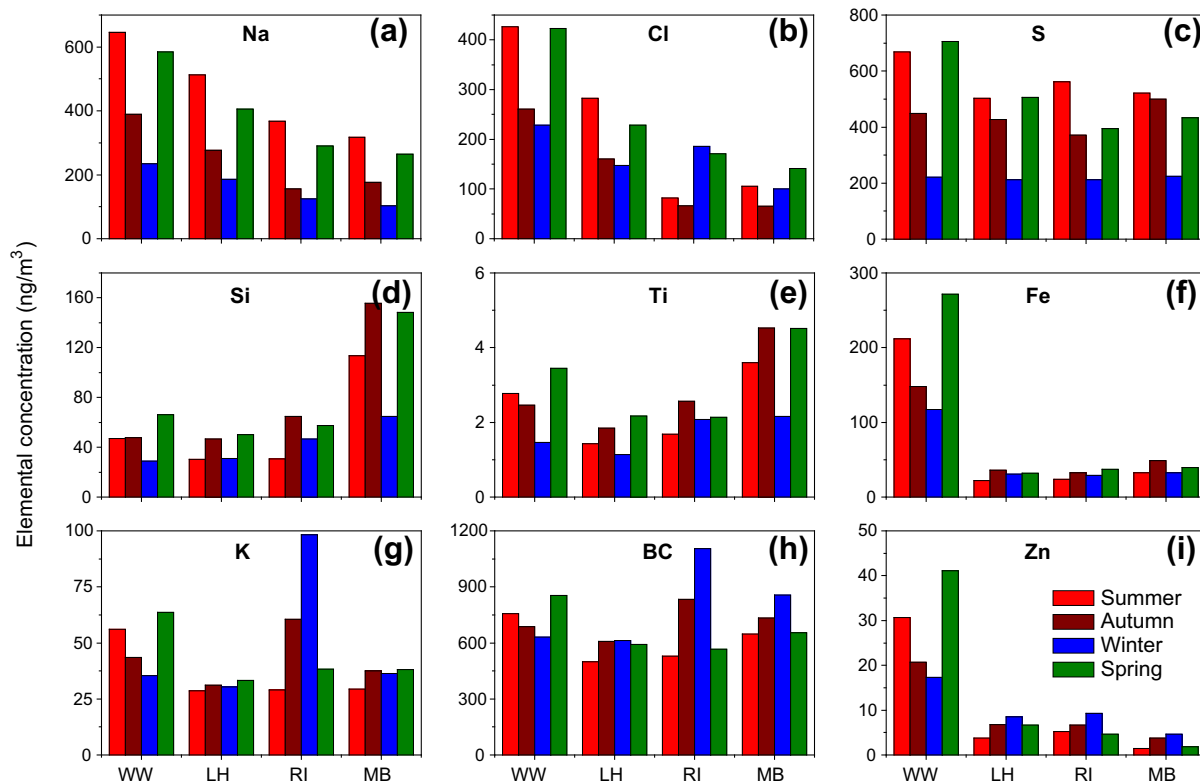


Fig. 9. Average seasonal concentrations of selected elements (ng/m³) at the four sites for summer (red), autumn (brown), winter (blue) and spring (green).

Table 2
Correlation coefficients of the elemental concentration of selected elements between pairs of sites, correlation coefficient >0.4 shaded.

Element	Site	Annual			Summer			Winter		
		WW	LH	RI	WW	LH	RI	WW	LH	RI
S	LH	0.82			0.72			0.72		
	RI	0.69	0.86		0.54	0.85		0.72	0.90	
	MB	0.42	0.57	0.66	0.27	0.33	0.46	0.53	0.74	0.89
Si	LH	0.83			0.78			0.82		
	RI	0.72	0.76		0.81	0.78		0.49	0.39	
	MB	0.38	0.32	0.35	0.49	0.65	0.56	0.47	0.23	0.47
K	LH	0.56			0.59			0.62		
	RI	0.20	0.40		0.42	0.42		0.37	0.70	
	MB	0.34	0.28	0.28	0.21	0.28	0.26	0.36	0.43	0.27
Na	LH	0.85			0.76			0.85		
	RI	0.63	0.70		0.41	0.45		0.67	0.78	
	MB	0.56	0.69	0.54	0.54	0.70	0.33	0.45	0.52	0.59
BC	LH	0.69			0.71			0.79		
	RI	0.24	0.44		0.34	0.36		0.55	0.58	
	MB	0.28	0.30	0.47	0.31	0.37	0.34	0.43	0.21	0.38
Radon	LH	0.91			0.81			0.94		
	RI	0.77	0.79		0.51	0.59		0.74	0.72	
	MB	0.67	0.66	0.69	0.53	0.60	0.39	0.52	0.48	0.68

Group 1 events occurred more frequently in summer and spring, whereas Group 2 events were most common in autumn and winter. Average aerosol mass and average elemental concentrations for these groups are presented in Table 4.

Total aerosol mass increased from Group 1 to Group 2 at all sites, confirming that majority of the aerosols observed had terrestrial origins. The observed relative mass change with fetch (Gp2/Gp1 ratio) was the least at WW and MB. Both of these sites are very close to strong point sources so changes in fetch may have a reduced influence due to the local mixing that occurs within each

Table 3
Seasonal mean radon (Bq/m³) at each site (derived only from days on which aerosol samples were available). Values can be compared to an activity of 0.1 Bq/m³, typical of "background" oceanic air [40].

	Warrawong	Lucas Heights	Richmond	Muswellbrook
Autumn	2.58	2.42	8.71	9.92
Winter	2.46	2.42	7.33	7.38
Spring	1.79	1.88	4.96	5.50
Summer	1.46	1.46	3.92	4.42

airshed. The largest ratio was at RI, consistent with a strong local aerosol source west of this site (most likely BC from domestic burning, supported by the high BC concentration).

Mostly, the Gp2/Gp1 ratio for marine markers (Na–Cl) decrease gradually from the coastal to inland sites. For Cl, however, the ratio was unexpectedly high at RI, which could be due to local sources of Cl (also identified in Section 3.1.2)

The Gp2/Gp1 ratio of soil markers (Si–Ti) was high at LH and RI, as expected with the contrast in terrestrial influence. The ratio was lower at WW, however, and lowest at MB, reflecting the influence of the local point sources on the seaward side of these sites. The low ratio at MB indicates that distant soil sources have a relatively low contribution at that site. It should be noted though that the transport of mineral dust and sea-spray depends not just on fetch, but on other factors such as wind speed [41,42].

The comparatively low ratios for BC and K at WW and MB highlight the existence of significant sources in the coastal regions east of these sites. The high ratios at RI emphasise the strong site-specific smoke sources west and south-west of this site.

The high Zn ratio at MB indicates that the Zn source lies to the west and south-west. The lower ratios of industrial markers at WW are consistent with the local industrial source. The majority of strongly stable nocturnal conditions (which would concentrate these emissions), occur in autumn and winter, when fetch is not

Table 4

Average concentration (ng/m³) of each marker element for Group 1 (mostly marine) and Group 2 (mostly terrestrial) aerosol samples, and the Group 2 / Group 1 ratio, at each site.

	Warrawong			Lucas Heights			Richmond			Muswellbrook		
	Gp1	Gp2	Ratio	Gp1	Gp2	Ratio	Gp1	Gp2	Ratio	Gp1	Gp2	Ratio
Mass	5305	7913	1.49	3443	6467	1.88	3468	11,088	3.20	4954	7159	1.45
Na	529	304	0.57	384	234	0.61	261	110	0.42	376	122	0.32
Cl	514	130	0.25	356	61	0.17	157	124	0.79	250	39	0.16
Si	32	71	2.22	12	70	5.83	14	91	6.50	114	176	1.54
Ti	2	4	2.00	1	3	3.00	1	4	4.00	3	5	1.67
K	43	61	1.42	21	43	2.05	26	120	4.62	30	50	1.67
BC	583	968	1.66	360	869	2.41	426	1322	3.10	534	915	1.71
S	392	619	1.58	254	508	2.00	281	387	1.38	414	438	1.06
Fe	160	279	1.74	22	44	2.00	15	44	2.93	29	59	2.03
Zn	29	35	1.21	4	11	2.75	4	11	2.75	1	5	5.00

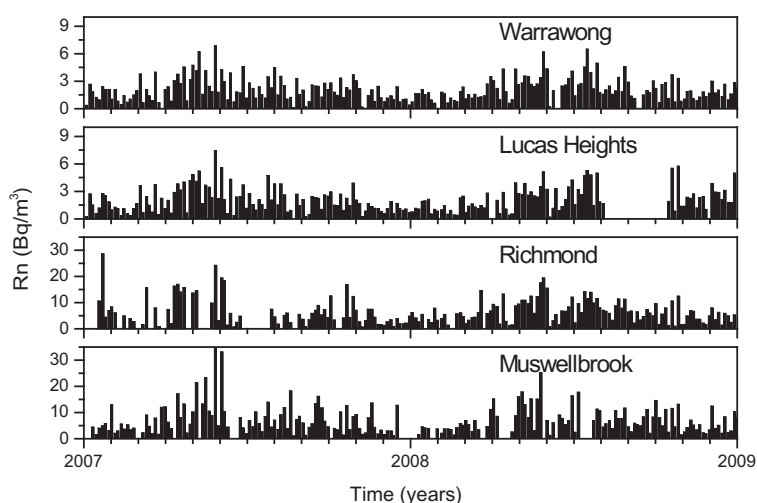


Fig. 10. Time series of daily mean radon concentration (Bq/m³), for those days of 2007 and 2008 on which aerosol samples were available, for the four sites. Note the difference in the y-scale for RI and MB.

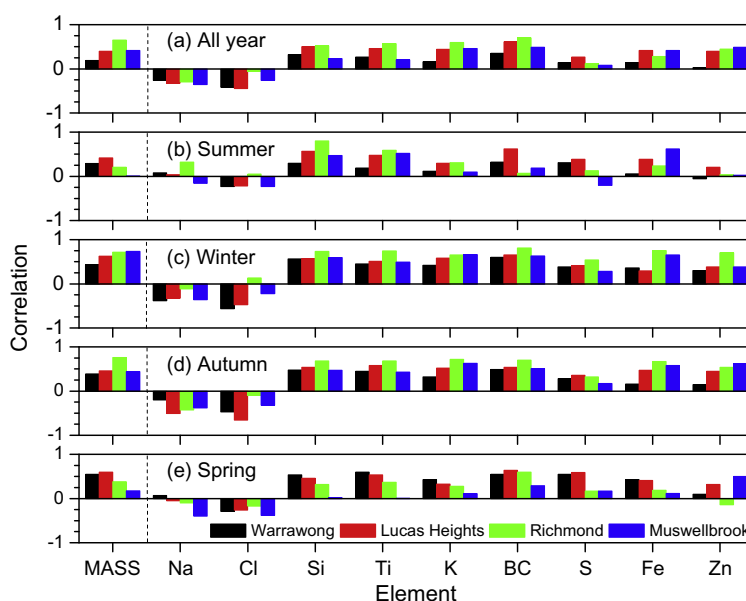


Fig. 11. Correlation coefficient between radon and elemental concentration of selected marker elements for all the data (a), summer only (b) winter only (c), autumn only (d) and spring only (e).

directly over the adjacent industrial complex. This could be why the Gp2/Gp1 ratio of industrial markers is low at WW.

Of the four sites, LH is expected to receive the lowest levels of urban/industrial emissions. LH exhibits the highest Gp2/Gp1 ratio

of secondary sulphate. The S delivered to this site under the strongest terrestrial influence is likely to be derived from distant precursor sources. Ratios are lower at all other sites, consistent with significant sources of secondary sulphate precursors in the more heavily urbanised coastal regions east of these sites.

3.7. Site specific correlation between radon and selected elements

Correlations between radon and the selected elements at a given site, calculated for those days on which aerosol measurements are available, are summarised in Fig. 11. The degree of correlation can be verified visually by comparing Fig. 10 with Figs. 4–8. Correlations of elements with radon can be interpreted in the following way: the sign of the correlation indicates whether the elemental source is primarily terrestrial (positive correlation) or oceanic (negative correlation), and the larger the correlation, the more similar the characteristics of the elemental source are to radon (i.e. widespread, spatially and temporally uniform). This is due to the terrestrial radon flux being about three orders of magnitude larger than the marine radon flux. Since air parcels analysed at the sites are, to various degrees, affected by both land and marine sources, the resulting radon signal is always dominated by the land component (see Section 3.2 and Table 1). Hence, a negative correlation between marine aerosols and radon is to be expected in all but few observations where the land component becomes relatively small with the corresponding correlation coefficient approaching zero. These two cases are illustrated by the correlation between radon and Na in Fig. 11c and in Fig. 11b, respectively.

For most elements a better correlation was seen in winter which indicated that in winter air masses pass over regions where the sources are spatially distributed and of more constant emission rate. In summer the best correlations with radon were with the soil markers. For most other elements though, correlations in summer are low, suggesting that sources in the urbanised coastal region east of the sites are variable either spatially and/or temporally. Spring is a time of mixed fetch and this was reflected with the low correlation of aerosols with radon (Fig. 11e).

The correlation of Si and Ti with radon for the entire data set is the lowest for MB indicating that the soil source was spatially and/or temporally variable. However, when seasonal correlation is examined, a higher correlation of Si and Ti in summer, winter and autumn indicated less variability in their sources for these seasons. The slightly lower correlation of Si and Ti with radon for summer in WW is consistent to the source being more variable during the summer fetch (see Fig. 2d). For the inland sites the lowest correlation was seen in spring whereas for LH there was a similar correlation for all seasons.

For K and BC the correlation was higher in winter when more distributed sources from domestic heating were present, whereas in summer the correlation was low for sites other than LH. At LH there was little seasonal difference in the correlation of K and BC with radon. From Section 3.1.3 the correlation of BC between sites was low which together with the current results indicates that the BC source is reasonably uniform locally to the site (other than in summer) but there is little mixing between sites.

Cl at RI shows a slight correlation with radon, which together with the results in Section 3.1.2 point to the possibility of a local source of Cl at RI.

Secondary sulfate (S) showed low correlations with radon at all sites indicating the possibility that the dominant sources are less distributed than the radon source.

Fe and Zn at WW showed low correlation with radon which was an indication of a spatially heterogeneous source and the low negative correlation in summer was due to the location of the industrial site to the east of the site, also supported by the higher average concentration recorded in summer (Fig. 9i).

The Rn-Mass correlation at WW was low but positive; indicating that the majority of aerosol mass at this site was of terrestrial origin. The low correlation indicated that the spatial and temporal source distribution of this aerosol mass was quite different to that of radon. A variable terrestrial based source of aerosol mass at WW was consistent with the nearby heavy industry.

RI showed a high, positive Rn-Mass correlation, indicative of a terrestrial based source that was spatially distributed and temporally constant and more so in winter. BC made up a large proportion of the RI aerosol mass.

The Rn-Mass correlation at LH was low indicating that the temporal and spatial distribution of sources was not uniform. At MB the overall Rn-Mass correlation was lower than that at RI, indicating that the dominant sources spatial and temporal distribution were not as uniform as at RI.

4. Conclusions

We have employed a new method to quantify the degree of spatial distribution and temporal consistency of PM_{2.5} terrestrial and marine sources using multi-elemental IBA techniques combined with radon gas measurements and correlation analysis.

Radon was well correlated with BC and K and particularly during winter when domestic heating constitutes a distributed source specific to the sites. However, in summer and spring the correlation of radon with BC and K was poor indicating that the distribution of these sources varies over the summer fetch region, with the exception of LH which showed similar correlation in summer and winter.

Radon was positively correlated with Si and Ti, but the correlation coefficient for the entire data set was smaller than for BC. For summer and winter, when fetch regions were constrained by the prevailing meteorology, Si and Ti showed good correlation with radon. Overall correlations between elements and radon were the smallest in spring, when a mixed fetch is represented.

Clear seasonal cycles were identified in many of the key marker elements, with the lowest S and Na concentrations in winter. Trends associated with the increasing distance of each site from the coast (3–130 km) were also characterised and discussed. Site-to-site correlation of the elements showed that Si was well correlated for three of the sites, indicative of a regional source for these sites (WW, LH and RI) and a site-specific source for the fourth site (MB). S was well correlated at all sites in winter. BC and K showed low correlation between sites indicative of site-specific sources.

Combining the site-to-site correlation results and the correlations between elements and radon at each site we can conclude that BC and K emissions are specific to the sites but within the sites they are distributed (for seasons other than summer). On the other hand Si and Ti are overall regional and distributed for LH, RI and WW (other than summer for WW), and for MB they are site-specific and variable. We have demonstrated that including radon in the analysis has given us the ability to quantify the degree of distribution of sources.

The above findings are typical for a large coastal city in the temperate zone where the lower atmosphere was affected by a range of natural and anthropogenic sources. Clearly the results detailed here for the Sydney region can be directly applied to other major urban and industrial areas with significant land sea interactions.

Acknowledgments

The NOAA Air Resources Laboratory (ARL) made available the HYSPLIT transport and dispersion model and the relevant input files for generation of back trajectories used in this paper. Assistance of Sylvester Werczynski, Ot Sisoutham, and Adrian Element

of ANSTO in the running of the radon experiment in the Sydney region is gratefully acknowledged.

Appendix A. Supplementary data

Supplementary data associated with this article can be found, in the online version, at doi:10.1016/j.nimb.2011.06.007.

References

- [1] National Pollution Inventory, 2010. <<http://www.npi.gov.au/>>.
- [2] T. Beer, M. Borgas, W. Bouma, P. Fraser, P. Holper, S. Torok, 2006. 'Atmosphere', theme commentary prepared for the 2006 Australia State of the Environment Committee, Department of Environment and Heritage, Canberra, <<http://www.environment.gov.au/soe/2006/publications/commentaries/atmosphere/index.html>>.
- [3] M. Hart, R. De Dear, R. Hyde, A synoptic climatology of tropospheric ozone episodes in Sydney, Australia, *Int. J. Climatol.* 26 (2006) 1635–1649.
- [4] Y.-C. Chan, D.D. Cohen, O. Hawas, E. Stelcer, R. Simpson, L. Denison, N. Wong, M. Hodge, E. Comino, S. Carswell, Apportionment of sources of fine and coarse particles in four major Australian cities by positive matrix factorisation, *Atmos. Environ.* 42 (2008) 374–389.
- [5] G.S. Hawke, D. Iverach, A study of high photochemical pollution days in Sydney, N.S.W. *Atmospheric Environment* 8 (1974) 597–608.
- [6] M. Azzi, G. Johnson, 1994. Photochemical smog assessment for NO_x emissions, using an IER-reactive plume technique. *Clean Air 1994 – Proceedings of the 12th International Conference of the Clean Air Society Australia and New Zealand*.
- [7] L.M. Leslie, M.S. Speer, Preliminary modelling results of an urban air quality model verifying the prediction of nitrogen dioxide, sulphur dioxide and ozone over the Sydney basin, *Meteorological and Atmospheric Physics* 87 (2004) 89–92.
- [8] X.L. Liu, N. Gao, P.K. Hopke, D. Cohen, G. Bailey, P. Crisp, Evaluation of spatial patterns of fine particle sulfur and lead concentrations in New South Wales, Australia, *Atmos. Environ.* 30 (1996) 9–24.
- [9] R.M. Leighton, E. Spark, Relationship between synoptic climatology and pollution events in Sydney, *Int. J. Biometeorol.* 41 (1997) 76–89.
- [10] H. Duc, I. Shannon, M. Azzi, Spatial distribution characteristics of some air pollutants in Sydney, *Mathematics and Computers in Simulation* 54 (2000) 1–21.
- [11] L. Corbyn, 2004. Future direction of air quality management in NSW. *Proceedings of NSW clean Air Forum*, 2004.
- [12] P. Gupta, S.A. Christopher, M.A. Box, G.P. Box, Multi year satellite remote sensing of particulate matter air quality over Sydney, Australia, *Int. J. Remote Sens.* 28 (2007) 4483–4498.
- [13] J.T. Hinkley, H.A. Bridgman, B.J.P. Buhre, R.P. Gupta, P.F. Nelson, T.F. Wall, Semi-quantitative characterisation of ambient ultrafine aerosols resulting from emissions of coal fires power stations, *Sci. Total Environ.* 391 (2008) 104–113.
- [14] J. Schwartz, D.W. Dockery, L.M. Neas, Is daily mortality associated specifically with fine particles?, *Journal of Air Waste Management Association* 46 (1996) 927–939.
- [15] City of Sydney 2010. <<http://www.cityofsydney.nsw.gov.au/Environment/GreenhouseAndAirQuality/CurrentStatus/AirPollution.asp>>.
- [16] D.D. Cohen, G.M. Bailey, R. Kondepudi, Elemental analysis by PIXE and other IBA techniques and their application to source fingerprinting of atmospheric fine particle pollution, *Nuclear Instruments and Methods* 109 (1996) 218–226.
- [17] D.D. Cohen, 1998, Characterisation of atmospheric fine particles using IBA techniques. *Nuclear Instruments and Methods in Physics Research*, B136–B138, 14–22.
- [18] D.D. Cohen, D. Garton, E. Stelcer, O. Hawas, Accelerator based studies of atmospheric pollution processes, *Radiat. Phys. Chem.* 71 (2004) 758–767.
- [19] D.D. Cohen, E. Stelcer, O. Hawas, D. Garton, IBA methods for characterisation of fine particulate atmospheric pollution: a local, regional and global research problem, *Nuclear Instruments and Methods in Physics Research B* 210–220 (2004) 145–152.
- [20] D.J. Jacob, M.J. Prather, P.J. Rasch, R.-L. Shia, Y.J. Balkanski, Evaluation and intercomparison of global atmospheric transport models using ²²²Rn and other short lived tracers, *J. Geophys. Res.* 102 (D5) (1997) 5953–5970.
- [21] M.H. Wilkening, W.E. Clements, Radon ²²²Rn from the ocean surface, *J. Geophys. Res.* 80 (1975) 3828–3830.
- [22] S.D. Schery, S. Huang, 2004. An estimate of the global distribution of radon emissions from the ocean, *Geophysical Research Letter*, Vol 31.
- [23] Y.J. Balkanski, D.J. Jacob, R. Arimoto, M.A. Kritz, Distribution of ²²²Rn over the North Pacific: implications for continental influences, *J. Atmos. Chem.* 14 (1992) 353–374.
- [24] H. Israel, Radioactivity of the Atmosphere, in: T.F. Malone (Ed.), *Compendium of Meteorology*, American Meteorological Society, Washington, DC, 1951, pp. 155–161.
- [25] G. Polian, G. Lambert, B. Ardouin, A. Jegou, Long-range transport of continental radon in subantarctic and arctic areas, *Tellus* 38B (1986) 178–189.
- [26] W. Zaborowski, S.D. Chambers, A. Henderson-Sellers, Ground based radon-222 observations and their application to atmospheric studies, *J. Environ. Radioactiv.* 76 (2004) 3–33.
- [27] J. Crawford, S. Chambers, D.D. Cohen, L. Dyer, T. Wang, W. Zaborowski, Receptor modelling using Positive Matrix Factorisation, back trajectories and Radon-222, *Atmos. Environ.* 41 (2007) 6823–6837.
- [28] J. Crawford, W. Zaborowski, D.D. Cohen, A new metric space incorporating radon-222 for generation of back trajectory clusters in atmospheric pollution studies, *Atmos. Environ.* 43 (2009) 371–381.
- [29] M. Chiaradia, B.E. Chenhall, A.M. Depers, B.L. Gulson, B.G. Jones, 1997. Identification of historical lead sources in roof dusts and recent lake sediments from an industrialized area: indications from lead isotopes, *The Science of the Total Environment*, 205 107–128.
- [30] E. Kim, P. Hopke, T. Lasron, N. Maykut, J. Lewtas, Factor analysis of Seattle fine particles, *Aerosol Sci. Technol.* 38 (2004) 724–738.
- [31] J.H. Seinfeld, S.N. Pandis, 1998. *Atmospheric Chemistry and Physics, From Air Pollution to Climate Change*, John Wiley and Sons, Inc., USA, ISBN 0-471-1-17816-0.
- [32] A.D. Griffiths, W. Zaborowski, A. Element, S. Werczynski, A map of radon flux at the Australian land surface. *Atmos. Chem. Phys.*, 10, 8969–8982, 2010 www.atmos-chem-phys.net/10/8969/2010/ doi:10.5194/acp-10-8969-2010.
- [33] W. Zhuo, Q. Guo, B. Chen, G. Cheng, 2008. Estimating the amount and distribution of radon flux density from the soil surface in China, *Journal of Environmental Radioactivity*, 99, 1143–1148, doi:10.1016/j.jenvrad.2008.01.011, 2008.
- [34] S. Whittlestone, W. Zaborowski, 1998. Baseline radon detectors for shipboard use: development and deployment in the first Aerosol Characterization Experiment (ACE 1), *Journal of Geophysical Research*, 103, 16743–16751.
- [35] C.F. Barrett, Correlation of smoke concentration in Great Britain, *International Association of Air and Water Pollution* 7 (1963) 991–993.
- [36] D.M. Elsom, Spatial correlation analysis of: air pollution data in an urban area, *Atmos. Environ.* 12 (1978) 1103–1107.
- [37] A.W. Keddie, G.W. Roberts, F.P. Williams, 1976. The application of numerical modelling to air pollution in the Forth Valley. In: C.A. Brebbia (Ed.), *Proceedings of International Conference on Mathematical Models for Environmental Problems*, Southampton, 1975. 183–199, Pentech Press, London.
- [38] R.R. Draxler, The accuracy of trajectories during ANATEX calculated using dynamic model analysis versus rawinsonde observations, *J. Appl. Meteorol.* 30 (1991) 1466–1467.
- [39] R.R. Draxler, G.D. Rolph, 2003. Hybrid Single-Particle Lagrangian Integrated Trajectory (HYSPLIT), model <<http://www.arl.noaa.gov/ready/hysplit4.html>>.
- [40] J.L. Gras, S. Whittlestone, Radon and CN: complementary tracers of polluted air masses at coastal and island sites, *Journal of Radio analytical and Nuclear Chemistry, Articles* 161 (1992) 293–306.
- [41] G. Wang, T. Wanquan, D. Mingyuan, Flux and composition of wind-eroded dust from different landscapes of an arid inland river basin in north-western China, *J. Arid Environ.* 58 (2004) 373–385.
- [42] S.I. Gong, L.A. Barrie, Modeling sea-salt aerosols in the atmosphere, *J. Geophys. Res.* 1002 (D3) (1997) 3805–3818.